MOLECULAR PHYSICS, 1986, VOL. 57, No. 4, 865–880

Collective excitations in an orientationally frustrated solid; neutron scattering and computer simulation studies of SF_6

by M. T. DOVE†‡, G. S. PAWLEY†, G. DOLLING§ and B. M. POWELL§

† Physics Department, University of Edinburgh, Edinburgh EH9 3JZ, Scotland

§ Atomic Energy of Canada Limited, Chalk River Nuclear Laboratories, Chalk River, Ontario K0J 1J0, Canada

(*Received 6 September 1985; accepted 28 October 1985*)

Collective excitations in the orientationally disordered phase of SF_6 have been studied by inelastic neutron scattering and molecular dynamics simulation techniques. Experimental measurements to observe acoustic modes were made along the high symmetry directions at temperatures of 100 K and 200 K. The excitations observed showed little evidence of discrete peaks but were all broad and overdamped. They showed little temperature dependence. The dynamical structure factors $S(\mathbf{Q}, \omega)$ calculated from the simulation are in qualitative agreement with the observed spectra but quantitatively show discrepancies. For smaller wave vectors than those studied experimentally the calculations show the existence of well-defined, long wavelength acoustic phonons. The wave vector at which the transition occurs between propagating and overdamped excitations was found to be temperature dependent. The results are interpreted in terms of the concept of orientational frustration. Some difficulties in the application of molecular dynamical simulation to the calculation of dynamical correlation functions are discussed in an Appendix.

1. INTRODUCTION

The phenomenon of orientational disorder (OD) in crystals has been known for many years, but it is only during the last decade that the microscopic nature of this disorder has been understood in any detail. An extensive review of the properties of OD solids has been given [1]. The advances in understanding have occurred partially as a result of the application of more powerful experimental techniques to the problem; for example, neutron scattering methods have proved particularly appropriate in the analysis of OD solids. But, in addition, experimental data can now be augmented by increasingly sophisticated computer simulation techniques, and because of increased computer capacity, molecular dynamics simulation (MDS) calculations can now provide realistic results for large systems of molecules with long-range order. However, most of the advances to date have

‡ Present address: Department of Theoretical Chemistry, University Chemical Laboratory, University of Cambridge, Lensfield Road, Cambridge CB2 1EW, England

been in understanding the 'static', time-averaged structure in simple OD solids; experimental measurements of the dynamical excitations in such crystals are few and their interpretation poorly understood.

The orientationally disordered phase of sulphur hexafluoride (SF_6) exists from its melting point at 223 K down to 96 K—a very wide temperature range. The structure of SF_6 at 100 K was investigated by Dolling *et al.* [2] using neutron powder diffraction methods, and they showed that the molecular centres of mass formed an ordered b.c.c. lattice. The S–F bonds were found to be preferentially aligned along the cubic axes, but the bond orientational distribution function had significant values as much as 20° away from these axes. The molecular site symmetry (O_h) was found to be the same as the molecular symmetry (unusual for an OD solid) and so molecular reorientations occur only between symmetrically equivalent orientations. Later measurements at 200 K showed the same qualitative features [3] but suggested a greater tendency for 'free' molecular rotation. Significant diffuse scattering was observed at 200 K and particular structure in this scattering was interpreted as evidence for orientational correlations.

These experimental results have been augmented by MDS calculations using a simple model for the interaction potentials in SF_6 [4, 5]. The calculations confirmed the nature of the S–F bond distribution function and showed that there are no orientational sites for the molecules other than those allowed by the O_h molecular symmetry. While the molecules were found to undergo rotational diffusion there did not appear to be any well-defined collective librational excitations. The molecules were shown to librate principally around the symmetry axes and to reorient frequently about one of these axes [5]. Calculations were made to study the correlations between the orientations of next-nearest neighbours in the lattice. It was demonstrated that the closest S–F bonds of these two molecules repel each other, and only rarely will two next-nearest neighbour molecules be orientationally ordered simultaneously [5]. This behaviour could be understood from a consideration of the interaction potential, and led to the development of the 'orientational frustration' model which is discussed in §4. It was shown that this orientational frustration is the origin of the orientational disorder in SF_6.

The orientational disorder in SF_6 is different in character from that found in other examples of OD solids. In many such crystals the molecules lie on sites which have a higher point group symmetry than the molecular symmetry itself. The disorder then arises because the molecules can dynamically reorient between two non-equivalent orientations. Examples of such crystals are the ammonium halides [6] and adamantane [7]. If the crystal has more than two non-equivalent orientations then the orientational disorder is more random in character. Examples are the alkali cyanides [8] and halogen-substituted methanes [2, 9]. If, in addition, the anisotropic orientational interactions are weak, the disorder closely approximates free molecular rotation. Examples are H_2 [10], CD_4 [11] and β-N_2 [12].

Inelastic neutron scattering measurements have been used to study the collective excitations in several of the crystals discussed above. The general features observed are that librational modes are overdamped so that there are no well-defined optic modes. Acoustic modes can usually be resolved for small wave vectors but also become overdamped away from the Brillouin zone centre. Several models have been proposed to interpret the collective excitations in OD crystals.

The most widely used is that of Michel and Naudts [13] who assumed rotational displacements of diffusive character and included terms in their hamiltonian to describe translational–rotational coupling. This model was developed to interpret the experimental temperature dependence of the elastic constants and also the inelastic neutron scattering data for KCN [13], and has also successfully explained neutron scattering results for both CBr_4 [9] and β-N_2 [12]. The model makes use of a mean-field approximation and so no explicit account is taken of direct orientational interactions arising from steric hindrance, and the model is therefore of limited use for SF_6. An alternative model which specifically included steric effects was developed by Coulon and Descamps [14]. It was used to interpret the diffuse scattering observed in the OD phase of CBr [15] but is a purely static model. Damien *et al.* [7] have interpreted the librational modes in adamantane in terms of a model which averaged over the different orientational configurations of a molecule in the cage of its near neighbours. This model thus included steric effects to some extent. The difficulties encountered in developing analytical models to describe the structures, phase transitions and collective excitations in OD crystals has led to the application of molecular dynamics simulations in an effort to understand these systems, and the MDS technique has been used to study the OD phases of β-N_2 [16], CH_4 [17], CCl_4 [18] and NaCN [19].

In the present paper we present the results of a study of the collective excitations in the OD phase of SF_6. Inelastic neutron scattering measurements of the excitations propagating along the major symmetry directions are compared directly with corresponding MDS calculations. As far as we are aware the present study is the first such detailed comparison of MDS calculations and experiment in an OD solid. The observed lineshapes are broad and generally featureless and, qualitatively at least, well described by the calculations. Several technical difficulties in calculating the relevant time correlation functions are discussed in detail. The study has highlighted several questions concerning the nature of collective excitations in orientationally frustrated OD solids.

2. Inelastic neutron scattering experiments

The single crystal of SF_6 was grown by condensing the gas into a quartz glass chamber and slowly cooling the liquid. The majority of measurements were made with the crystal at 200 K but some data were obtained at 100 K in order to investigate the temperature dependence of specific modes. The crystal volume was ≈ 8 cm^3 and its mosaic spread was $\approx 0{\cdot}8°$. The crystal was oriented with $[1\bar{1}0]$ vertical so that the three high symmetry directions were accessible in the experimental scattering plane.

The inelastic neutron scattering measurements were made on the L3 and C5 triple-axis spectrometers at the NRU reactor, Chalk River. The majority of measurements were made with Ge (113) and graphite (0002) as the monochromator and analyser respectively, and collimations before and after the specimen were $0{\cdot}59°$ and $0{\cdot}72°$ respectively. A fixed analysing frequency of 3·5 THz was used for most of the measurements, and the spectrometer resolution in this configuration was 0·21 THz. Several scans were made with higher resolution (0·15 THz) and although there is some evidence for rather more structure at this resolution, the essential features of the observed lineshapes are unchanged. Since previous neutron scattering measurements on OD solids have indicated that collective librational excitations do not exist, and since the recent MDS calculations on SF_6

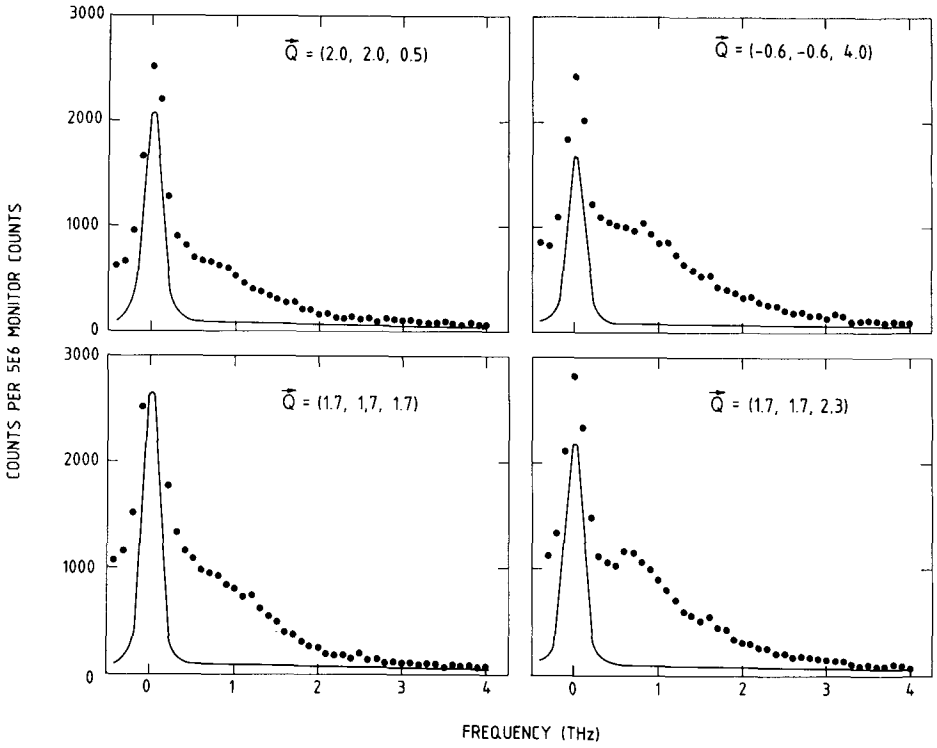

Figure 1. Experimental scattered neutron distributions from SF_6 at 200 K. The filled circles show the raw data and the solid line shows the background from the empty container. The components of the scattering vector **Q** shown for each distribution are in units of $2\pi/a$, where a is the lattice parameter.

[4, 5] have indicated this to be also the case here, the present measurements concentrated on the predominantly translational excitations. Observations were thus made along all three symmetry directions in both 'longitudinal' and 'transverse' configurations in zones in which it was expected that translational phonons would be observed. Some typical scattered neutron distributions at 200 K are shown in figure 1. All four distributions show an intense generally featureless scattering at low frequencies. There is some evidence of discrete structure in the distributions, but all are much broader than the experimental resolution, which is defined by the elastic peak in the background scattering. There were only minimal changes in the form of the neutron distributions at different neutron momentum transfers and the data shown in figure 1 are typical of the complete set of measurements. The measurements at 100 K did not differ in any essential way from those at 200 K.

The present data on SF_6 are in contrast to similar measurements on other OD solids. The acoustic modes in CD_4 [11] are generally well-defined, while in adamantane only the librational modes showed significant broadening [7]. In CBr_4 [9] the acoustic modes were also well-defined, although their intensity decreased rapidly with increasing wave vector. For β-N_2 [12] the translational

phonons are well defined at small wave vector, although they were observed on a large background which was interpreted as an overdamped librational mode. At larger wave vectors these translational phonons broaden and weaken. The measurements suggest a significant temperature dependence in the intensity from the overdamped librational mode, in contrast to the present data for SF_6.

3. Molecular dynamics simulation

3.1. *'Experimental' details*

The technique of molecular dynamics simulation is well suited to the study of the dynamical properties of condensed matter, and its application to a wide range of studies of simple molecular crystals has recently been reviewed [20]. In the present application of MDS to SF_6 the crystal is represented by the model developed in previous calculations [4, 5, 21], with the intermolecular potential between two SF_6 molecules represented by a pair-wise Lennard-Jones interaction acting between the fluorine atoms. Only interactions between nearest and next-nearest neighbour molecules in the b.c.c. lattice were explicitly included, so the model is as simple as possible, while retaining enough essential features for the overall behaviour of the model to resemble closely that of the real SF_6 crystal. The calculations were performed on the ICL Distributed Array Processor (DAP) at the University of Edinburgh. The DAP is a parallel processor which has a 64×64 two-dimensional array of connected processing elements with hard-wired periodic boundary facilities. In order to exploit this feature it is necessary to map the real 3-D lattice onto the 2-D hardware grid of the DAP and this necessitates the use of a parallelopiped shape for the MDS sample [22]. The finite sample size means that it is not possible to make calculations at arbitrarily selected wave vectors, while the sample shape does not allow the calculations to be made along symmetry directions. However, since the simulation sample contains 4096 molecules, the density of accessible points in wave vector space is so large that it is always possible to find an accessible wave vector close to any specified wave vector. The sample axes used in the present simulation and the 64 wave vectors at which calculations were made are given in Appendix A. The simulations modelled ensembles with constant energy and volume. The equations of motion were solved by the Beeman [23] algorithm using discrete time steps of 0·005 ps, and the simulation calculations were carried out for 16 000 time steps. This large number was chosen by consideration of the accuracy of the calculated scattering function. The components of the density operator $b(\mathbf{Q}, t)$ (see below) were calculated and stored every ten time steps; these calculations were carried out during the running of the simulation rather than using the procedure of storing configurations and performing the calculations as a later, second operation [4]. Simulations were made at temperatures of 115 K and 200 K and at densities corresponding to zero pressure. The calculated lattice parameters were 5·7604 Å and 5·8589 Å respectively. The corresponding experimental values are 5·78 $\pm$ 0·01 Å [2] and 5·913 $\pm$ 0·001 Å [3]. The small differences between the observed and calculated lattice parameters suggest that the model potential is slightly softer than the true potential in SF_6 [4], but it has been shown that, nevertheless, the model is a good representation of real SF_6.

3.2. *Calculation of correlation functions*

The theoretical formalism appropriate to neutron scattering experiments has been given by Dolling *et al.* [2] and the essential expressions are summarized here for convenience. The time dependent density operator $b(\mathbf{Q}, t)$ is the Fourier transform of the instantaneous scattering length density of the crystal

$$b(\mathbf{Q}, t) = \sum_{j\mu} b_{j\mu} \exp [i\mathbf{Q} \cdot \mathbf{r}_{j\mu}(t)], \tag{1}$$

where $\hbar\mathbf{Q}$ is the neutron momentum transfer for scattering vector $\mathbf{Q}$, $b_{j\mu}$ the coherent neutron scattering length of atom μ in molecule j, and $\mathbf{r}_{j\mu}(t)$ the instantaneous position vector of atom $j\mu$ defined as

$$\mathbf{r}_{j\mu}(t) = \mathbf{R}_j + \mathbf{u}_j(t) + \mathbf{x}_{j\mu}(t)$$

where $\mathbf{R}_j$ is the time averaged position vector of the centre of mass of molecule j, $\mathbf{u}_j(t)$ the instantaneous displacement of the centre of mass of molecule j, and $\mathbf{x}_{j\mu}(t)$ the instantaneous position vector of atom μ relative to the centre of mass of molecule j. The intermediate scattering function $F(\mathbf{Q}, t)$ is the time autocorrelation function of the density operator

$$F(\mathbf{Q}, t) = \langle b(\mathbf{Q}, 0) b^+(\mathbf{Q}, t) \rangle \tag{2}$$

where $\langle\ \rangle$ represent a thermodynamic average. In an MDS calculation the thermodynamic average is replaced by a time average over the sample configurations:

$$F(\mathbf{Q}, t) = \lim_{t \to \infty} \frac{1}{T} \int_0^T b(\mathbf{Q}, \tau) b^+(\mathbf{Q}, t + \tau)\, d\tau. \tag{3}$$

The dynamical structure factor, $S(\mathbf{Q}, \omega)$, which is the quantity measured in a neutron scattering experiment, is the time Fourier transform of the intermediate scattering function

$$S(\mathbf{Q}, \omega) = \frac{1}{2\pi} \int F(\mathbf{Q}, t) \exp(-i\omega t)\, dt, \tag{4}$$

where $\hbar\omega$ is the neutron energy transfer. The structure of the SF_6 molecule is such that if the neutron scattering length of the fluorine atoms is set to zero so that only scattering from the sulphur atom is included, then the motion of the molecular centre of mass alone is probed. Consequently we can define a centre of mass density operator $b_{\mathrm{cm}}(\mathbf{Q}, t)$ by

$$b_{\mathrm{cm}}(\mathbf{Q}, t) = \sum_j b_{\mathrm{s}} \exp [i\mathbf{Q} \cdot (\mathbf{R}_j + \mathbf{u}_j(t))] \tag{5}$$

and corresponding centre of mass functions $F_{\mathrm{cm}}(\mathbf{Q}, t)$ and $S_{\mathrm{cm}}(\mathbf{Q}, \omega)$ can be calculated. In this way the centre of mass motions can be separated from the librational motions in MDS calculations.

3.3. *Intermediate scattering function*

The intermediate scattering function $F(\mathbf{Q}, t)$ was evaluated from the simulation calculations using equation (3), although it would have been significantly faster to have calculated $F(\mathbf{Q}, t)$ by a Fourier transform method

$$B(\mathbf{Q}, \omega) = \int b(\mathbf{Q}, t) \exp(i\omega t)\, dt, \tag{6}$$

$$F(\mathbf{Q}, t) = \int |B(\mathbf{Q}, \omega)|^2 \exp(i\omega t)\, d\omega. \tag{7}$$

However, we found that $F(\mathbf{Q}, t)$ was excessively 'noisy' when calculated by the latter method, even when the transforms were performed using smoothing filters. Since the source of the 'noise' could not be identified when using equations (6) and (7), the 'time-averaging' method of equation (3) was preferred. Equation (3) is strictly true only in the limit $T \rightarrow \infty$, but in general practice T is chosen to be just long enough to give adequate averaging over the time steps. This will correspond to several periods of oscillation of $F(\mathbf{Q}, t)$, and this non-ideal time averaging will itself lead to statistical noise in the calculated correlation function.

The MDS calculation is purely classical and hence $F(\mathbf{Q}, t)$ has time reversal symmetry and, ideally, is real. Since the density operator is itself complex, in practice the intermediate scattering function has a small imaginary component, whose magnitude may be used as a measure of the statistical noise in $F(\mathbf{Q}, t)$. The amplitude of the imaginary component increases gradually from a value of zero at $t = 0$; since the calculated $F(\mathbf{Q}, t)$ usually decays rapidly with time, its imaginary part finally becomes similar in magnitude to the amplitude of the long-time tail of the real part of $F(\mathbf{Q}, t)$. A more general discussion of the accuracy of the calculations is given in Appendix B. In the present calculation $F(\mathbf{Q}, t)$ was evaluated for $t = 0 \rightarrow 5$ ps and the averaging time T was taken to be 75 ps. In the few cases where $F(\mathbf{Q}, t)$ did not decay until times longer than 5 ps it was evaluated for $t = 0 \rightarrow 20$ ps and T was taken as 60 ps.

The intermediate scattering function was calculated for 64 scattering vectors along the symmetry directions investigated in the neutron scattering measurements, and these are given in Appendix A. The total function $F(\mathbf{Q}, t)$ and the centre of mass function $F_{cm}(\mathbf{Q}, t)$ were calculated at both temperatures. Some typical results are shown in figure 2. It can be seen that a common feature of the functions shown is that $F(\mathbf{Q}, t)$ decays rapidly to the noise level before the first node in the oscillation of the function. This feature was found for all the symmetry directions and was independent of whether the mode was of longitudinal or transverse character provided the reduced wave vector was not too small (see below). The lifetime of $F(\mathbf{Q}, t)$ is too short for well-defined excitations to be established and, qualitatively, this explains why the experimental neutron groups shown in figure 1 are so featureless. Three of the centre of mass functions also rapidly decay so that even the expected translational acoustic modes are overdamped. The similarity to the behaviour of the total function suggests strong translational–orientational coupling. Only for the calculation at $\mathbf{Q} = (0{\cdot}232, 0{\cdot}018, 0{\cdot}226)$ does $F_{cm}(\mathbf{Q}, t)$ not decay before the first node. This value of $\mathbf{Q}$ is the smallest of the reduced wave vectors shown in figure 2.

In figure 3 the function $F_{cm}(\mathbf{Q}, t)$ is shown for the smallest computationally accessible reduced wave vectors $\zeta(= \mathbf{q}/\mathbf{q}_{max})$ at both temperatures. In contrast to

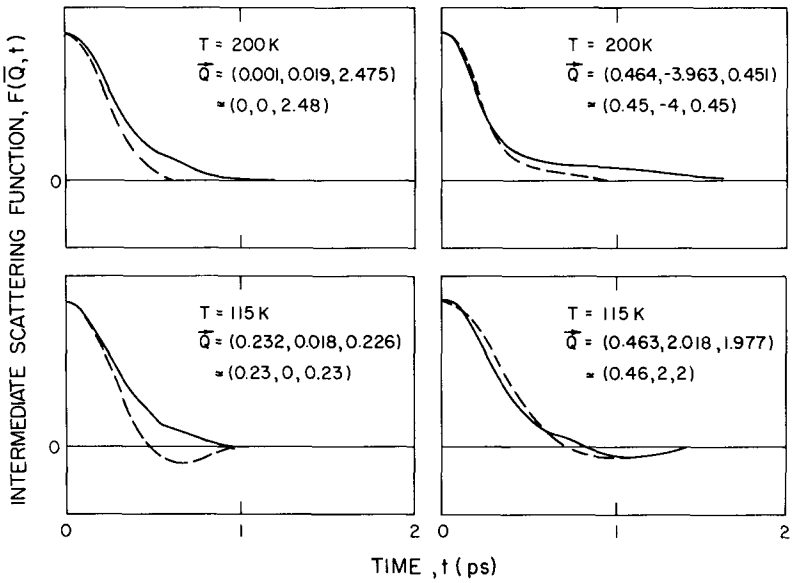

Figure 2. Intermediate scattering function, $F(\mathbf{Q}, t)$, calculated as a function of time by MDS at temperatures of 200 K and 115 K. The components of the scattering vector, $\mathbf{Q}$, are in units of $2\pi/a$. The symbol = shows the scattering vector for which the simulation was actually made while the symbol $\simeq$ shows the nearest momentum transfer that lies on one of the symmetry directions. The solid line shows the total $F(\mathbf{Q}, t)$ while the dashed line shows its centre of mass component $F_{cm}(\mathbf{Q}, t)$.

the functions shown in figure 2, these have a well-defined oscillation with a long lifetime. The same characteristic is seen in $F(\mathbf{Q}, t)$, but $F_{cm}(\mathbf{Q}, t)$ is shown for clarity since this excludes the librational component. The long lived oscillation suggests that close to the zone centre the acoustic modes are well-defined and this effect was found for all symmetry directions. The calculated form of $F(\mathbf{Q}, t)$ is thus strongly wave vector dependent. For small ζ, as ζ increases, the lifetime of

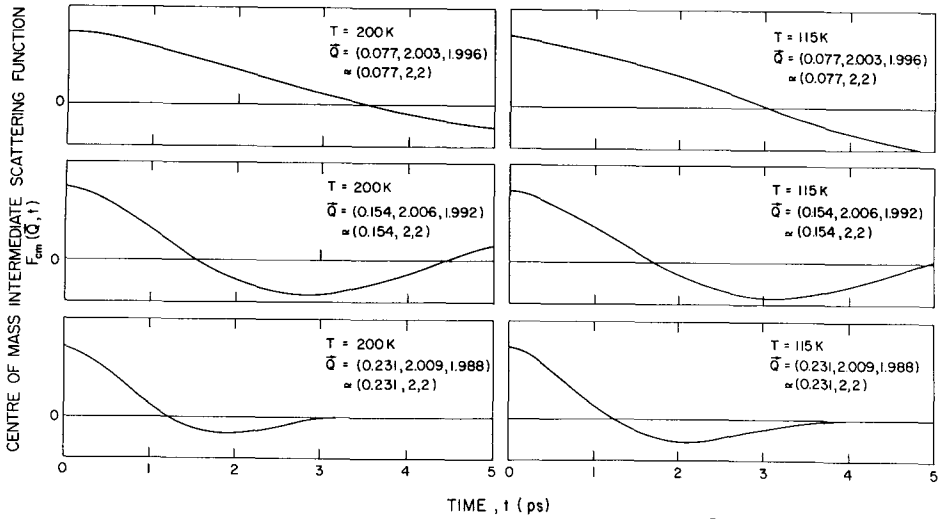

Figure 3. The centre of mass intermediate scattering function, $F_{cm}(\mathbf{Q}, t)$, calculated for three small reduced wave vectors, ζ, along [100] near the reciprocal lattice point (022) at 200 K and 115 K.

$F(\mathbf{Q}, t)$ decreases markedly, but for $\zeta \geqslant 0{\cdot}25$ the lifetime is approximately independent of ζ. The principal effect of temperature is shown in figure 3. In this regime of small ζ, $F(\mathbf{Q}, t)$ is strongly temperature dependent with the damping increasing with temperature. For wave vectors far from the centre of the Brillouin zone (i.e. large ζ) temperature appears to have little effect.

3.4. *Dynamical structure factor*

The dynamical structure factor $S(\mathbf{Q}, \omega)$ is the Fourier transform of the intermediate scattering function (see equation (4)). It was found that the Fourier transform operation converted oscillatory noise in the long-time tail of $F(\mathbf{Q}, t)$ into peaks in $S(\mathbf{Q}, \omega)$ which are probably spurious. To avoid this uncertainty we truncated $F(\mathbf{Q}, t)$ at the time t_0 at which the function has decayed to the level of the statistical noise, as discussed above. From figure 2 it is clear that t_0 is rather small for most $\mathbf{Q}$ values (as low as 0·75 ps in some cases) and this leads to a poorly defined scattering function, since the Fourier transform operation produces points in the frequency domain with spacing $\Delta\omega = 2\pi/t_0$. This difficulty is overcome by setting $F(\mathbf{Q}, t) = 0$ for $t > t_0$ up to a time corresponding to the required frequency interval in $S(\mathbf{Q}, \omega)$. It should be noted that this procedure is purely interpolative and does not affect the inherent resolution of the Fourier transform. However, in the present case filling $F(\mathbf{Q}, t)$ with zeros in the range $t_0 < t \leqslant 2\pi/\Delta\omega$ is not simply a computational convenience but is a good approximation to the real situation since $F(\mathbf{Q}, t)$ appears really to be zero in that range. The time reversal symmetry of $F(\mathbf{Q}, t)$ is exploited by setting $F(\mathbf{Q}, -t) = F(\mathbf{Q}, t)$ and the complete intermediate scattering function extending from $-2\pi/\Delta\omega \leqslant t \leqslant 2\pi/\Delta\omega$ is then transformed to produce $S(\mathbf{Q}, \omega)$. Despite this elaborate treatment of the Fourier transform operation we cannot entirely eliminate the possibility that some of the structure in the calculated $S(\mathbf{Q}, \omega)$ may be spurious. Since the MDS calculation is classical, the calculated scattering is symmetrical in frequency, i.e. $S(\mathbf{Q}, \omega) = S(\mathbf{Q}, -\omega)$. The true quantum mechanical function does not possess this symmetry property, and in order to give the quantum mechanical characteristics to the MDS function we use the Schofield [24] approximation and, following Klein *et al.* [16], multiply the latter function by $\exp(\hbar\omega/2k_B T)$. The dynamical structure factors calculated from the $F(\mathbf{Q}, t)$ of figure 2 are shown in figure 4, together with the corresponding $S_{cm}(\mathbf{Q}, \omega)$. For three $\mathbf{Q}$ values both $S(\mathbf{Q}, \omega)$ and $S_{cm}(\mathbf{Q}, \omega)$ are very similar in form, the major difference being the higher frequency tail in the former function. This similarly again suggests that the centre of mass motion is strongly coupled to the orientational disorder. These three calculated $S(\mathbf{Q}, \omega)$ show a broad, generally featureless peak centred at $\omega = 0$, in qualitative agreement with experiment (see § 4). The calculation for the smallest reduced wave vector shows a significant difference between $S(\mathbf{Q}, \omega)$ and $S_{cm}(\mathbf{Q}, \omega)$. The former function shows the broad, featureless peak centered at $\omega = 0$, but the latter function shows a broad peak at a non-zero value of ω. This results from the 'oscillation' in the corresponding $F_{cm}(\mathbf{Q}, t)$ shown in figure 2.

3.5. *Comparison with experiment*

The most detailed neutron scattering measurements were made at 200 K with $\mathbf{Q} = 2\pi/a$ (003) $\rightarrow 2\pi/a$ (004) and $\mathbf{Q} = 2\pi/a$ (004) $\rightarrow 2\pi/a$ ($-0{\cdot}5$, $-0{\cdot}5$, 4). Calculations of the observed lineshapes were made for scattering vectors as close to

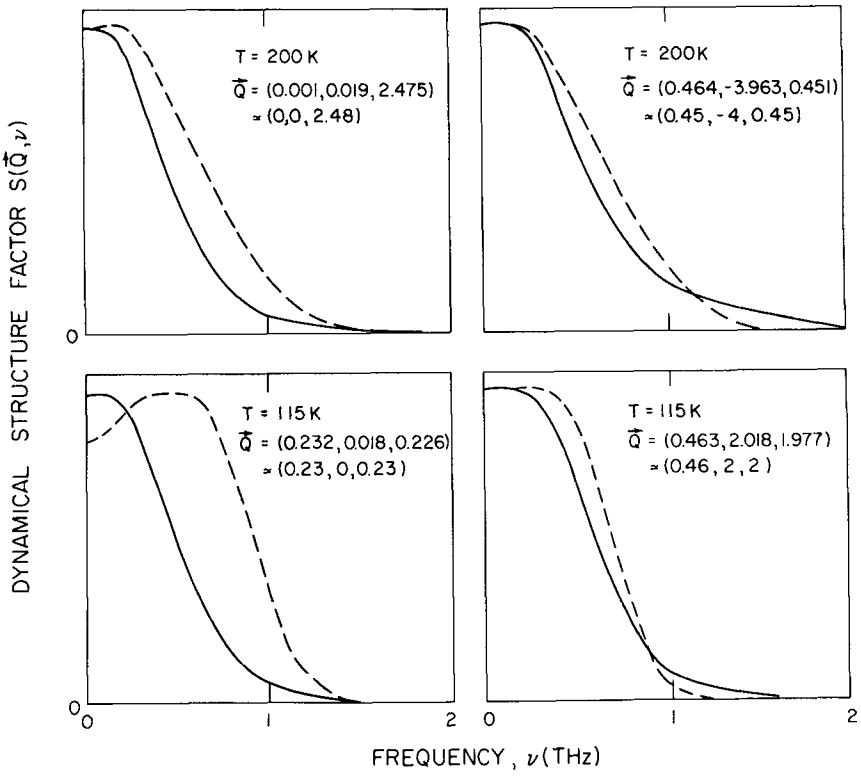

Figure 4. The dynamical structure factor, $S(\mathbf{Q}, \nu)$ ($2\pi\nu = \omega$) calculated from the intermediate scattering functions shown in figure 2.

these as the MDS sample shape allowed (Appendix A). The experimental neutron cross section is given in [2] as

$$\frac{d^2\sigma}{d\Omega\, d\varepsilon} \approx \frac{k}{k_0} S(\mathbf{Q}, \omega), \tag{8}$$

where $\mathbf{k}_0(\mathbf{k})$ are the incident (scattered) neutron wave vectors. The experimental measurements were made with fixed k and with a monitor which corrected for the factor $1/k_0$. The observed intensity is thus directly proportional to $S(\mathbf{Q}, \omega)$. The calculated $S(\mathbf{Q}, \omega)$ is convoluted with the experimental resolution function determined from the width of the vanadium elastic incoherent scattering. The 'experimental' dynamical structure factor is then directly comparable with the corresponding calculated function. The two distributions are normalized by making the maxima in the observed and calculated functions equal. The observed and calculated $S(\mathbf{Q}, \omega)$ are then compared in figure 5 for eight scattering vectors along the [001] and [110] directions.

It is clear the agreement between the observed and calculated lineshapes is qualitatively good, but there are discrepancies in both peak intensities and frequencies in a detailed quantitative comparison. In general the calculation shows more structure than is observed. This may be due to the use of an oversimplified experimental resolution function for the convolution procedure, but, as discussed previously (see § 3.4, also Appendix B), the transformation to obtain $S(\mathbf{Q}, \omega)$ may

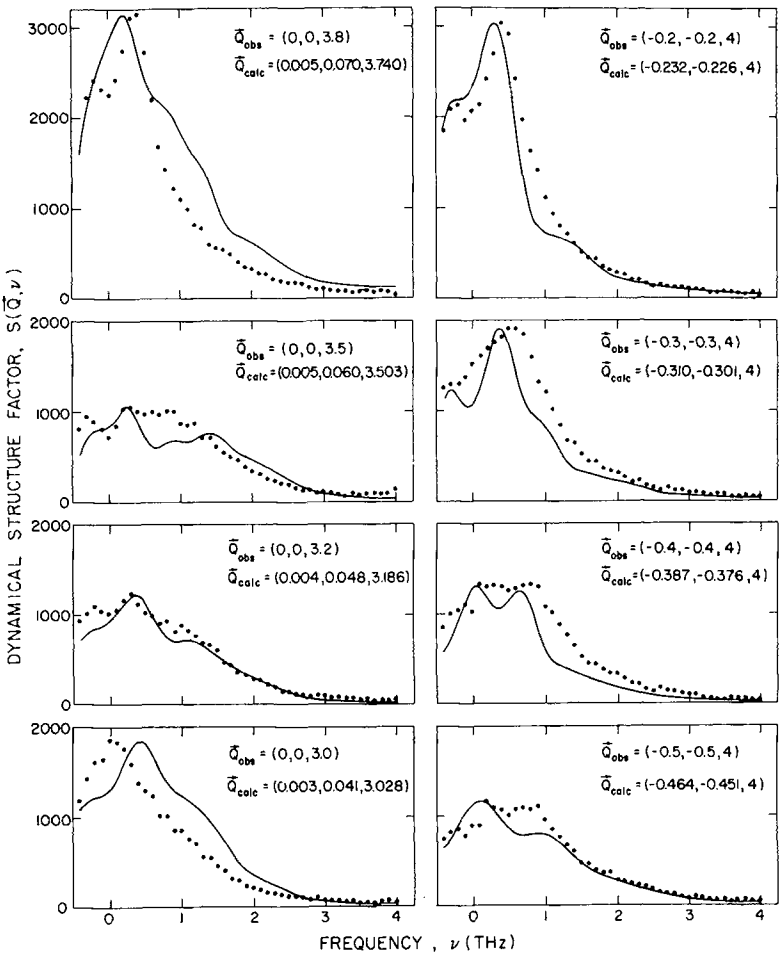

Figure 5. Comparison of observed and calculated dynamical structure factors for scattering vectors along the symmetry directions [001] and [110] near the reciprocal lattice point (004). The filled circles show the background subtracted data. The line shows the calculated function after convolution with the experimental resolution. $\mathbf{Q}_{obs}$ is the experimental momentum transfer while $\mathbf{Q}_{calc}$ is that for which the calculation is made.

itself artificially produce structure in the function. For momentum transfers at which the calculation shows two broad, but partially separated peaks only a single very broad peak is usually observed, while for momentum transfers at which the calculation shows a single strong peak this is usually not at the observed frequency. The latter momentum transfers are for small wave vectors and the discrepancies between the observed and calculated frequencies may reflect the fact that the model potential is rather softer than the true potential. It may also be partly due to the calculation being made for wave vectors not identical to the experimental ones. Despite these discrepancies, the overall agreement between observed and calculated $S(\mathbf{Q}, \omega)$ in such an extensive and detailed comparison shows that MDS is a powerful method for understanding collective excitations in OD phases.

4. Discussion

The present inelastic scattering measurements have shown that well-defined collective excitations do not exist in SF_6, and even the translational acoustic modes are overdamped at the wave vectors investigated. This is true for all three high symmetry directions. Furthermore, this characteristic is temperature independent; the data at 100 K are remarkably similar to those at 200 K. Attempts were made to fit the lineshapes at 200 K with the Michel–Naudts theory [13] and with a damped harmonic oscillator model. However, although either of these models can be fitted reasonably well to the lineshapes at specific wave vectors, the fitted parameters for a sequence of wave vectors did not vary in a consistent manner. This behaviour contrasts with the successful interpretation of data for β-N_2 in terms of the Michel–Naudts theory [12]. The lineshapes derived from the present MDS calculations for SF_6 are in qualitative agreement with those observed for all 64 experimental wave vectors. This suggests that the interpretation of the orientational disorder in terms of orientational frustration [5] is a valid description.

The concept of frustration, while common in solid state and statistical physics has not previously been introduced in molecular physics. Calculations of the interactions between two SF_6 molecules as functions of separation for different relative orientations have shown that when the molecules are aligned along the crystal axes the forces between nearest neighbour molecules are strongly attractive whereas those between next-nearest neighbours are repulsive. Thus there is a competition between these interactions: nearest neighbour interactions favour orientational ordering while next-nearest neighbour interactions oppose this ordering. At high temperatures this frustration is resolved dynamically so that the lattice remains of high symmetry and the molecules are dynamically disordered. But at low temperatures, when the molecules no longer have enough kinetic energy to relieve the frustration dynamically, the crystal undergoes a phase transition in which the unit cell distorts in order to accommodate the increase in orientational order. It is thus the orientational frustration that is the direct cause of the orientational disorder. The distinction between 'typical' OD crystals and orientationally frustrated ones is that in the former every molecule resides in one of a finite number of symmetry related orientations or is randomly oriented, whereas in the latter the competition between the intermolecular interactions prevents neighbouring molecules from simultaneously being ordered.

Dove and Pawley [5] show that this effect is distinct from the disorder caused by thermal motions and fluctuations. These authors have also explained that there is little temperature dependence to be associated with the orientational frustration, unlike the case of thermal motion. The lack of significant temperature dependence in SF_6 is thus in agreement with an 'orientational frustration' interpretation. The only effect of temperature in the simulation is to reduce the wave vector decay constant, which is consistent with the greater rotational freedom of the molecules at higher temperatures. It should be noted that in this model there is no need to ascribe any of the behaviour to the direct effects of anharmonicity. The orientational frustration will give rise to the same effect if the intermolecular interactions are harmonic, because different molecules will experience different (harmonic) forces due to the disorder. This is in contrast to the common concept of an OD crystal as a 'highly anharmonic' solid.

We have discussed the present experimental results in terms of the concept of orientational frustration. A possible alternative interpretation might be that the

crystal consists of long-lived low-symmetry clusters of ordered molecules. Within each cluster the intermediate scattering function might then be long-lived. But because the clusters have different orientations relative to the crystal axes and also may have different sizes, a specified momentum transfer **Q** for the crystal will apparently be a different **Q**-value for each cluster. Consequently, for a specified **Q**-value of the crystal the net $F(\mathbf{Q}, t)$ will be a superposition of the functions from individual clusters at the same time but different **Q** values. This average might then appear as a rapidly decaying function even though each contribution is itself long-lived. However, graphics displays of the time-dependent molecular trajectories calculated by MDS have recently shown that long-lived, low-symmetry clusters do not exist [25]. The disorder in SF_6 is found to be completely dynamic and fully consistent with our interpretation in terms of orientational frustration.

The present study shows that further work is necessary to obtain a more quantitative understanding of the effects of orientational frustration on the lattice dynamics. In particular, measurements of the excitation spectrum at smaller wave vectors than those studied in the present experiment are necessary to observe the existence of well-defined acoustic modes, to measure the wave vector decay constant and to measure the elastic constants for comparison with existing calculations [26]. The detailed distribution of the diffuse scattering in a single crystal of SF_6 should also be measured. Powder diffraction measurements at 200 K [3] have shown that diffuse scattering is intense at this temperature, and a preliminary MDS calculation which separated the scattering into different components has already been made [5]. Since the concept of orientational frustration may apply to many OD crystals, the development of a better theoretical model, that transcends the limitations of those discussed in this paper, would be highly desirable.

Two authors (M. T. Dove and G. S. Pawley) thank SERC (U.K.) for financial support and one author (B. M. Powell) thanks The Royal Society of London for supporting a stay in Edinburgh during which the calculations were made.

Appendix A

The method of mapping a three dimensional periodically repeating lattice onto a two-dimensional square grid with cyclic boundary conditions has been described in detail by Pawley and Thomas [22]. For a b.c.c. lattice, a roughly cubic sample can be set up defined by the following lattice vectors:

$$\mathbf{X} = (13, -1, 0)a,$$

$$\mathbf{Y} = (-0{\cdot}5, 12{\cdot}5, -0{\cdot}5)a,$$

$$\mathbf{Z} = (0{\cdot}5, 3{\cdot}5, 12{\cdot}5)a,$$

where a is the length of the b.c.c. unit cell edge. We transform this cell to one that corresponds to a string of 4096 molecules so that

$$\mathbf{X} = (4096, 0, 0)a,$$

$$\mathbf{Y} = (13, -1, 0)a,$$

$$\mathbf{Z} = (168{\cdot}5, -0{\cdot}5, -0{\cdot}5)a.$$

The corresponding reciprocal lattice is then defined by the three vectors

$$\mathbf{X}^* = (1, 13, 324)/4096a,$$

$$\mathbf{Y}^* = (0, -1, 1)/a,$$

$$\mathbf{Z}^* = (0, 0, -2)/a.$$

The density operator $b(\mathbf{Q}, t)$ has been evaluated for the following four sets of scattering vectors:

(1) $\mathbf{Q} \approx 002 \rightarrow 004 = j\mathbf{X}^* - \mathbf{Z}^*, j = 0 - 25$

$= 002 + j(1, 13, 324)/4096,$

(2) $\mathbf{Q} \approx 0\bar{4}1 \rightarrow 1\bar{4}1 = j(317\mathbf{X}^* + \mathbf{Y}^* + 13\mathbf{Z}^*) + 4\mathbf{Y}^* + 2\mathbf{Z}^*, j = 0 - 12$

$= 0\bar{4}0 + j(317, 25, 308)/4096,$

(3) $\mathbf{Q} \approx 101 \rightarrow 202 = j(317\mathbf{X}^* + \mathbf{Y}^* + 13\mathbf{Z}^*), j = 13 - 24$

$= j(317, 25, 308)/4096,$

(4) $\mathbf{Q} \approx 022 \rightarrow 122 = j(316\mathbf{X}^* + \mathbf{Y}^* + 13\mathbf{Z}^*) - 2\mathbf{Y}^* - 3\mathbf{Z}^*, j = 0 - 12$

$= 022 + j(316, 12, -16)/4096.$

The maximum deviations from the four specified symmetry directions are then 4, 8, 8 and 5 per cent respectively.

Appendix B

As described in § 3.3, although $F(\mathbf{Q}, t)$ calculated by MDS is, in principle real, in practice an imaginary component exists because of the imperfect averaging defined in equation (3). We define $F'(\mathbf{Q}, t)$ and $F''(\mathbf{Q}, t)$ to be the real and imaginary components of $F(\mathbf{Q}, t)$. As described in the text, for SF_6 at wave vectors that are not close to the Brillouin zone centre, $F'(\mathbf{Q}, t)$ decays very rapidly to zero. Thus the only significant part of the function is in the region $t \simeq 0$.

By definition, in the limit $t \rightarrow 0$, $F(\mathbf{Q}, t) \rightarrow 1$ and the noise in $F(\mathbf{Q}, t)$, i.e. $F''(\mathbf{Q}, t) \rightarrow 0$. In general it was observed that the amplitude of $F''(\mathbf{Q}, t)$ rises gradually from zero as t increases until it becomes equal to the long-time tail of the over-damped form of $F'(\mathbf{Q}, t)$. This time varied according to the value of $\mathbf{Q}$, but in general was of the order of 1 ps or less. There appears to be a significant structure in the form of $F''(\mathbf{Q}, t)$, corresponding to strong oscillations in the frequency range 0·5–1 THz. This is particularly evident in the calculation of $F(\mathbf{Q}, t)$ for the smallest allowed wave vectors. Figure 6 shows the two components of $F(\mathbf{Q}, t)$ for the centre of mass motion corresponding to a longitudinal acoustic vibration. At this wave vector it is clear that $F'(\mathbf{Q}, t)$ exhibits a well defined oscillation corresponding to a slightly damped harmonic acoustic phonon, and this is accompanied by a corresponding oscillation of $F''(\mathbf{Q}, t)$ out of phase by $\pi/2$. This behaviour indicates problems concerning thermal averaging and ergodicity that are inherent in the standard MDS method. It is generally assumed that the MDS sample is a true microcanonical ensemble and thus truly ergodic, with effective random, but correctly weighted, sampling of configurational phase space. Thus greater accuracy can be obtained in the calculation simply by allowing the simulation to proceed for a longer time, with the noise being purely statistical and arising from the coarse averaging of the whole of phase space.

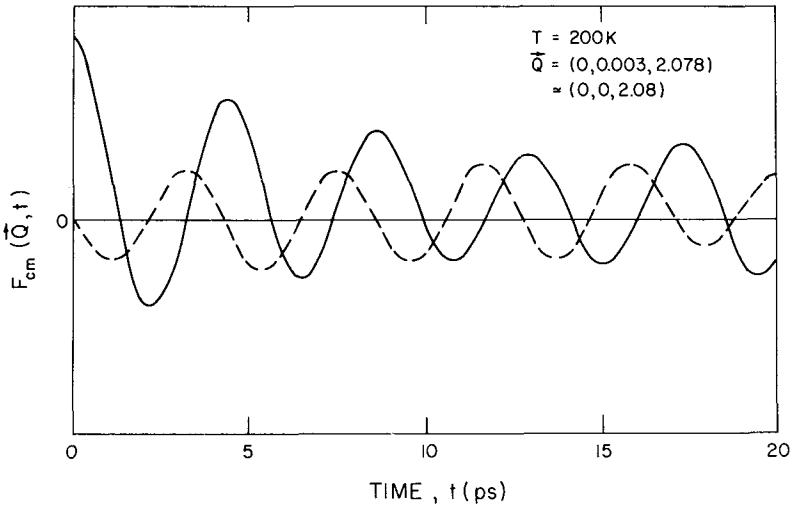

Figure 6. Time dependence of the real (———) and imaginary (– – – –) components of the centre of mass intermediate scattering function calculated for a small reduced wave vector ($\zeta = 0{\cdot}08$) along [001].

While this may be approximately correct for many calculations, the behaviour of the noise in $F(\mathbf{Q}, t)$ shown in figure 6 suggests that in certain cases it is incorrect, since $F''(\mathbf{Q}, t)$ follows a pure sinusoidal variation that is clearly not at all random. The amplitude of $F''(\mathbf{Q}, t)$ did not vary with the number of time steps used in the averaging procedure (equation 3) in a simple way. Calculations made with averaging times of 30, 45 and 60 ps did not reveal any systematic behaviour of the amplitude with the number of time steps; and at larger times the amplitude of $F''(\mathbf{Q}, t)$ always remained just less than that of $F'(\mathbf{Q}, t)$. It appears that the amplitude of $F''(\mathbf{Q}, t)$ will not be reduced to a negligible value by averaging over any simulation time lengths that are practical from a computational viewpoint, and in fact it is not clear that it will reduce to zero at all. Thus true ergodicity and hence also true thermodynamic ensemble averaging may not be attainable in this case. This behaviour is not simply due to equilibrium problems: the configurations used as starting points in the correlation function calculations correspond to 36 000 and 60 000 time steps for the two runs at 115 and 200 K respectively.

The non-ergodicity is probably due to the effects of using small finite-sized samples with periodic boundary conditions. It is clear that there exists a critical time for the MDS sample, t_c, given by $t_c = L/v_s$ where L is a linear dimension of the MDS sample and v_s is the sound velocity. This critical time is that taken for any 'disturbance' to propagate around the sample through the periodic boundary conditions and interact with itself. Thus any time correlation function representing non-localized motions will be perturbed by this self-interaction over times of the order of t_c. For a longitudinal acoustic mode with $q = 1/L$ and with linear dispersion, the critical time $t_c = 1/\nu$, where ν is the frequency of that mode. For the smallest allowed wave vector this critical time corresponds to just one period of oscillation.

It appears from figure 6 that a possible effect of the existence of t_c is that in the case of the lowest order vibrational mode the self-interactions act as a feedback mechanism that enhances the correlation function $F(\mathbf{Q}, t)$ at large times,

such that the system is effectively 'ringing' with a well-defined frequency. In view of the lack of understanding of the effects of this artificial 'self-interaction' we believe that the detailed form of $F(\mathbf{Q}, t)$ is probably not reliable for $t > t_c$ at these wavevectors. Thus the form of the resultant $S(\mathbf{Q}, \omega)$ should also be treated with caution. The resonant frequencies will probably be correct but the line widths will be unreliable. These observations are of general application and are particularly relevant for the smaller sample sizes (e.g. 100 to 200 particles) typically employed in MDS. In these cases the smallest allowed wave vector would be a large fraction of the dimension of the Brillouin zone and the 'ringing' effect discussed above may yield significant artefacts in the calculated forms of $S(\mathbf{Q}, \omega)$ for these wave vectors. Fortunately in the present study at wave vectors far from the Brillouin zone centre $F(\mathbf{Q}, t)$ decays in a time less than t_c, so that the feedback is not so significant and the self-interaction affects only the noise in $F(\mathbf{Q}, t)$, i.e. $F''(\mathbf{Q}, t)$.

References

[1] Sherwood, J. N. (editor), 1979, *The Plastically Crystalline State* (John Wiley & Sons).

[2] Dolling, G., Powell, B. M., and Sears, V. F., 1979, *Molec. Phys.*, **37,** 1859.

[3] Powell, B. M., Sears, V. F., and Dolling, G., 1982, *Neutron Scattering*, 1981, edited by J. Faber, Jr. (A.I.P. Conference Proceedings No. 89).

[4] Dove, M. T., and Pawley, G. S., 1983, *J. Phys.* C, **16,** 5969.

[5] Dove, M. T., and Pawley, G. S., 1984, *J. Phys.* C, **17,** 6581.

[6] Press, W., Eckert, J., Cox, D. E., Rotter, C., and Kamitakahara, W., 1976, *Phys. Rev.* B, **14,** 1983.

[7] Damien, J. C., Lefebvre, J., More, M., Hennion, B., Currat, R., and Fouret, R., 1978, *J. Phys.* C, **11,** 4323. See also Windsor, C. G., Saunderson, D. M., Sherwood, J. N., Taylor, D., and Pawley, G. S., 1978, *J. Phys.* C, **11,** 1741.

[8] Price, D. L., Rowe, J. M., Rush, J. J., Prince, E., Hincks, E. G., and Susman, S., 1972, *J. chem. Phys.*, **56,** 3697. Rowe, J. M., Hincks, D. G., Price, D. L., Susman, S., and Rush, J. J., 1973, *J. chem. Phys.*, **58,** 2039.

[9] More, M., and Fouret, R., 1980, *Faraday Discuss.*, **69,** 75.

[10] Sullivan, N. S., and Devoret, M., 1978, *J. Phys. Paris*, **39,** (C6), 92.

[11] Press, W., 1972, *J. chem. Phys.*, **56,** 2597. Stirling, W. G., Press, W., and Stiller, H., 1977, *J. Phys.* C, **10,** 3959.

[12] Powell, B. M., Dolling, G., and Nieman, H. F., 1983, *J. chem. Phys.*, **79,** 982.

[13] Michel, K. H., and Naudts, J., 1978, *J. chem. Phys.*, **68,** 216.

[14] Coulon, G., and Descamps, M., 1980, *J. Phys.* C, **13,** 2847.

[15] More, M., Lefebvre, J. Hennion, B., Powell, B. M., and Zeyen, C. M. E., 1980, *J. Phys.* C, **13,** 2833.

[16] Klein, M. L., and Weis, J-J., 1977, *J. chem. Phys.*, **67,** 217. Klein, M. L., Lévesque, D., and Weis, J-J., 1981, *J. chem. Phys.*, **74,** 2566.

[17] Bounds, D. G., Klein, M. L., and Patey, G. N., 1980, *J. chem. Phys.*, **72,** 5348.

[18] McDonald, I. R., Bounds, D. G., and Klein, M. L., 1982, *Molec. Phys.*, **45,** 521.

[19] Lynden-Bell, R. M., McDonald, I. R., and Klein, M. L., 1983, *Molec. Phys.*, **48,** 1093.

[20] Pawley, G. S., and Dove, M. T., 1983, *Helv. phys. Acta*, **56,** 583. Pawley, G. S., Brass, A. M., Dove, M. T., and Refson, K., 1985, *J. Chim. phys.*, **82,** 249.

[21] Pawley, G. S., 1981, *Molec. Phys.*, **6,** 1321.

[22] Pawley, G. S., and Thomas, G. W., 1982, *J. comput. Phys.*, **47,** 165.

[23] Beeman, D., 1976, *J. comput. Phys.*, **20,** 130.

[24] Schofield, P., 1960, *Phys. Rev. Lett.*, **4,** 239.

[25] Dove, M. T., Fincham, D., and Hubbard, R., 1986, *J. molec. Graphics* (in the press).

[26] Dove, M. T., and Pawley, G. S., 1986 (in preparation).